Multi-Objective Optimization of a Minimal Cardiac Model to Replicate ToR-ORd Behavior

Mayra Urbieta Barbosa[1], Joventino O Campos[1], Rodrigo W dos Santos[1]

[1] Federal University of Juiz de Fora, Juiz de Fora, Brazil

Abstract

Complex cardiac models like the ToR-ORd are essential for arrhythmia research but are computationally demanding. We optimized the four-variable Bueno-Orovio model to replicate the electrophysiological behavior of the 44-variable ToR-ORd model, focusing on action potential duration (APD90), maximum upstroke velocity (max dV/dt), and waveform morphology. Sobol-based global sensitivity analysis identified the 13 most influential parameters for optimization. We employed the NSGA-II algorithm to manage three conflicting objectives: minimizing errors in the dynamic restitution curves of APD90 and max dV/dt, as well as in the overall waveform morphology. Analysis of the resulting Pareto front enabled selection of a balanced solution representing the optimal compromise among objectives. This calibrated model achieves an 11-fold reduction in computational complexity and 25-fold speedup on numerical simulations, demonstrating that simplified models can accurately reproduce essential cardiac dynamics with superior computational performance for large-scale simulations.

1. Introduction

Computational modeling is an essential tool for investigating cardiac arrhythmias, a primary cause of global mortality [1]. While detailed biophysical models like the ToR-ORd [2] provide high physiological fidelity, their computational expense—requiring the solution of 44 coupled ordinary differential equations with simulation times exceeding hours for tissue-scale studies—limits their feasibility for large-scale simulations [3]. This creates a critical need for computationally efficient alternatives that retain essential physiological accuracy.

Phenomenological models, such as the four-variable Bueno-Orovio minimal model [4], offer a promising solution by representing ionic currents through simplified mathematical functions rather than detailed biophysical mechanisms. However, their utility depends on rigorous calibration to ensure they replicate the behavior of their detailed counterparts. This study presents a systematic methodology to optimize the Bueno-Orovio model to reproduce key electrophysiological properties of the ToR-ORd model, specifically waveform morphology and the APD90 and max dV/dt restitution curves—critical determinants of conduction velocity, wavefront stability, and arrhythmic substrate formation [5].

The problem was formulated as a multi-objective optimization problem, using the NSGA-II algorithm to manage conflicting objectives of simultaneously matching action potential duration, maximum depolarization rate, and overall waveform morphology. NSGA-II's ability to handle non-convex Pareto fronts makes it particularly suitable for cardiac model optimization where trade-offs between electrophysiological properties are inherently non-linear. This methodology provides a systematic framework for minimal model calibration with validation demonstrating computational feasibility for tissue-scale arrhythmia studies.

2. Methods

The workflow involved calibrating the Bueno-Orovio minimal model to replicate the electrophysiological behavior of the detailed ToR-ORd model, using a global sensitivity analysis to identify key parameters followed by multi-objective optimization.

2.1. Cardiac Electrophysiology Models

2.1.1. The ToR-ORd Reference Model

The reference data was generated by the ToR-ORd human ventricular model [2], a system of 44 ordinary differential equations (ODEs) that provides a high-fidelity representation of ionic currents and intracellular dynamics.

2.1.2. The Bueno-Orovio Minimal Model

The Bueno-Orovio model [4] phenomenologically describes the action potential with four state variables. Its

formulation was adapted to directly represent the membrane potential (V_m) in mV through the linear transformation $V_m = \alpha \cdot u - V_o$, where u is the original dimensionless variable, $\alpha = 122.6589$ is the scaling factor, and $V_o = -88.637$ mV corresponds to the resting potential. The transformed model is governed by:

$$\frac{dV_m}{dt} = \alpha \cdot [-(J_{fi} + J_{so} + J_{si}) + I_{stim}(t)] \quad (1)$$

$$\frac{dv}{dt} = \frac{(1 - H(V_m, \theta_v)) \cdot (v_{inf} - v)}{\tau_v} - \frac{H(V_m, \theta_v) \cdot v}{\tau_{v+}} \quad (2)$$

$$\frac{dw}{dt} = \frac{(1 - H(V_m, \theta_w)) \cdot (w_{inf} - w)}{\tau_w} - \frac{H(V_m, \theta_w) \cdot w}{\tau_{w+}} \quad (3)$$

$$\frac{ds}{dt} = \frac{1}{\tau_s}\left[\frac{1 + \tanh(k_s \cdot ((V_m + V_o) - u_s))}{2} - s\right] \quad (4)$$

where J_{fi}, J_{so}, and J_{si} are the fast inward, slow outward, and slow inward currents.

2.1.3. Target Electrophysiological Properties

The optimization aimed to match three key electrophysiological properties across basic cycle lengths (BCLs) from 300 to 900 ms at 50 ms intervals:

- **Action Potential Duration (APD90):** Time for 90% repolarization.
- **Maximum Upstroke Velocity (max dV/dt):** Peak rate of depolarization.
- **Waveform Morphology:** Overall action potential shape, evaluated at BCL = 500 ms.

Action potentials were simulated using 1 ms current pulses applied at intervals corresponding to each BCL, with 8 beats per BCL and measurements taken from the final pulse to ensure steady-state conditions.

2.2. Sensitivity Analysis

To reduce the dimensionality of the optimization problem, we performed a global sensitivity analysis using the Sobol method [6]. This variance-based technique identified the influence of each of the model's 28 parameters on the outputs. The total-order index (S_T) was calculated, which captures a parameter's direct effect plus all interaction effects [7]. The 13 parameters with $S_T > 0.1$ for at least one target metric were selected for optimization, with parameter bounds set to ±50% of original values, reducing the search space.

2.3. Multi-Objective Optimization

The calibration was defined as a multi-objective optimization problem to handle the conflicting nature of simultaneously matching different electrophysiological properties.

2.3.1. Objective Functions

We aimed to simultaneously minimize three normalized error functions:

1. **APD90 Error (E_{APD})-** The normalized RMS error for the APD90 restitution curve:

$$E_{APD}(\mathbf{x}) = \sqrt{\frac{1}{\mathbf{N}}\sum_{\mathbf{i=1}}^{\mathbf{N}}\left(\frac{\mathbf{APD_{sim,i}} - \mathbf{APD_{ref,i}}}{\mathbf{\bar{A}\bar{P}D_{ref}}}\right)^{\mathbf{2}}} \quad (5)$$

2. **Max dV/dt Error (E_{dVdt})-** The normalized RMS error for the max dV/dt restitution curve:

$$E_{dVdt}(\mathbf{x}) = \sqrt{\frac{1}{\mathbf{N}}\sum_{\mathbf{i=1}}^{\mathbf{N}}\left(\frac{\mathbf{V'_{max,sim,i}} - \mathbf{V'_{max,ref,i}}}{\mathbf{\bar{V}'_{max,ref}}}\right)^{\mathbf{2}}} \quad (6)$$

3. **Waveform Morphology Error (E_{forma})-** The RMSE between voltage traces, normalized by the RMS of the reference:

$$E_{forma}(\mathbf{x}) = \frac{\text{RMSE}(\mathbf{V_{sim}}, \mathbf{V_{ref}})}{\text{RMS}(\mathbf{V_{ref}})} \quad (7)$$

where $\mathbf{x}$ is the parameter vector, N is the number of BCLs, and V'_{max} denotes max dV/dt.

2.3.2. NSGA-II Algorithm

We used the Non-dominated Sorting Genetic Algorithm II (NSGA-II) [8], an evolutionary algorithm that identifies a set of optimal trade-off solutions, known as the **Pareto front**. From the final front, we selected the best-compromise solution as the one with the minimum Euclidean distance to the ideal objective vector [0, 0, 0].

2.4. Numerical Implementation

The model and optimization were implemented in Python. Simulations were accelerated approximately 25-fold by combining the LSODA adaptive ODE solver from SciPy with Just-in-Time (JIT) compilation via Numba [9]. The NSGA-II algorithm was implemented using the PyMOO library [10] with a population of 50 individuals evolved over 50 generations until convergence.

3. Results

3.1. Sensitivity Analysis

The Sobol analysis was performed on the APD90 and max dV/dt restitution curves to identify the most influential parameters. Initial analysis revealed that parameters

affecting waveform morphology were identical to those influencing APD90, justifying the focus on restitution curves for sensitivity assessment. Figure 1 displays the total-order (S_T) indices, highlighting the high sensitivity of parameters like θ_w, τ_{si}, and u_s.

The analysis identified 15 out of 28 parameters with significant influence ($S_T > 0.1$). However, based on the expected physiological ranges from the ToR-ORd target data, the initial (u_o) and final (u_u) voltage values were predefined and excluded from optimization. This resulted in 13 parameters selected for optimization: u_{so}, τ_{w+}, τ_{so1}, w^*_{inf}, τ_{v1-}, τ_{v+}, τ_{si}, τ_{fi}, u_s, k_s, k_{so}, τ_{w1-}, and θ_w.

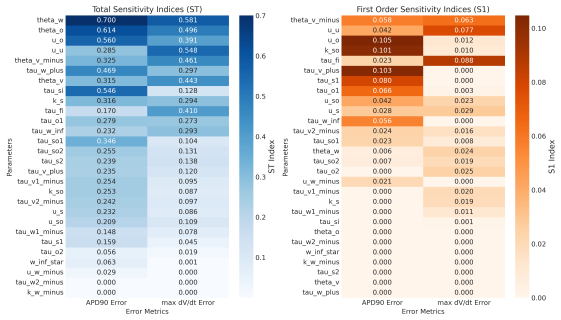

Figure 1. Sobol sensitivity analysis heatmaps. Total-order (S_T, left) and first-order (S_1, right) indices for the APD90 and max dV/dt error metrics. Warmer colors indicate higher sensitivity.

3.2. Multi-Objective Optimization

The NSGA-II algorithm converged to a Pareto front of 51 non-dominated solutions, representing the optimal trade-offs among the three error objectives (Figure 2). Analysis of 2D projections revealed the most significant conflict exists between minimizing APD90 error and waveform morphology error (Figure 3). This structural trade-off is explained by the initial sensitivity analysis, which showed that both objectives are controlled by the same set of influential parameters, making simultaneous optimization inherently conflicting.

3.3. Performance of the Calibrated Model

The selected optimization run provides a satisfactory balance across all objectives. The final performance metrics are summarized in Table 1, corresponding to below 3% average relative error across all targets. The calibrated model achieves an 11-fold reduction in computational complexity (4 vs 44 variables) and demonstrates a 25-fold speedup in simulation time compared to the ToR-ORd model. The optimization process required 3.9 hours runtime.

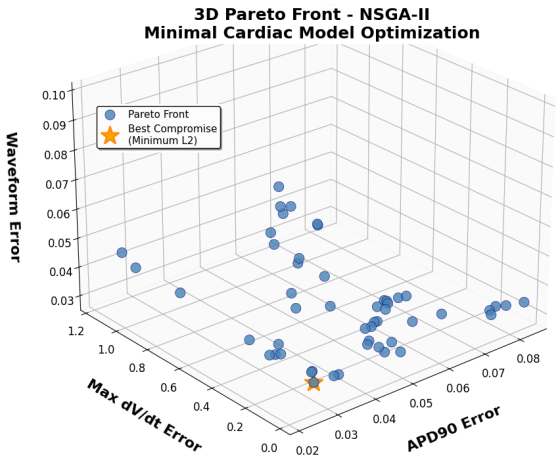

Figure 2. The 3D Pareto front from the NSGA-II optimization. Each point is a non-dominated solution. The highlighted star indicates the selected best-compromise solution.

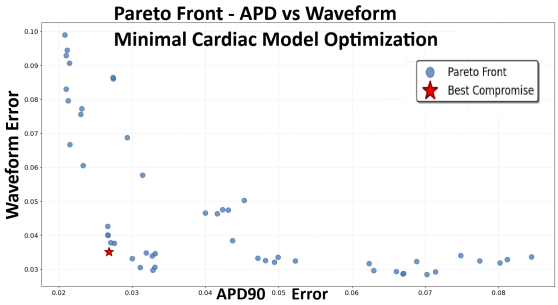

Figure 3. 2D projection of the Pareto front showing the trade-off between APD90 and waveform morphology errors. The highlighted point represents the selected best-compromise solution.

Table 1. Performance metrics of the optimal model selected from the Pareto front.

Metric	Value
APD90 Error (E_{APD})	0.027
max dV/dt Error (E_{dVdt})	0.011
Waveform Error (E_{forma})	0.035
Optimization Time (Hours)	3.9

Qualitatively, the calibrated model shows high fidelity, where its action potential morphology closely matches the ToR-ORd reference (Figure 4). Crucially, the model accurately reproduces the restitution curves for both APD90 and max dV/dt across the full range of BCLs (Figure 5), confirming its ability to capture the heart's dynamic rate-dependent behavior.

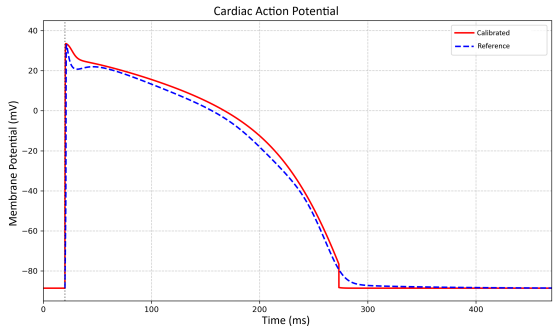

Figure 4. Action potential of the final calibrated model (solid red) compared to the ToR-ORd reference (dashed blue) for a BCL of 500 ms.

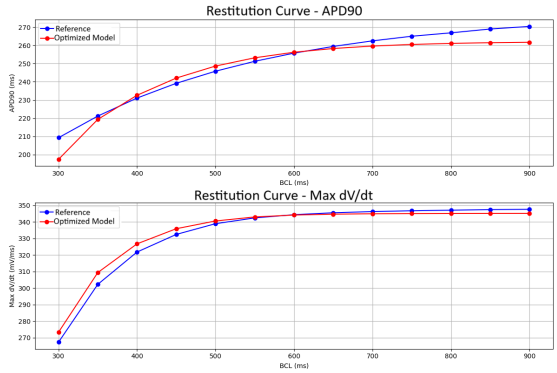

Figure 5. Restitution curves of the final model (red) and the reference (blue) for APD90 (top) and max dV/dt (bottom), demonstrating excellent agreement.

4. Conclusions

This study successfully optimized a 4-variable minimal model to replicate the 44-variable ToR-ORd model with below 3% average relative error. The calibrated model achieves an 11-fold reduction in computational complexity and 25-fold speedup while preserving essential electrophysiological properties. Pareto front analysis quantified fundamental trade-offs between APD90, max dV/dt, and morphology, providing a systematic framework for model selection. The model shows reduced accuracy at very short BCLs, limiting its application in high-frequency arrhythmia studies. Future work should focus on improving restitution curve fitting at short cycle lengths to enhance tachyarrhythmic modeling capabilities.

Acknowledgments

The authors would like to express their thanks to Minas Gerais State Research Support Foundation (FAPEMIG) - PCE-00048-25; APQ-02752-24, APQ-02445-24, APQ-02513-22, FINEP (SOS Equipamentos 2021 AV02 0062/22), Conselho Nacional de Desenvolvimento Científico e Tecnológico (CNPq) Proc. 423278/2021-5 and 310722/2021-7; Coordenação de Aperfeiçoamento de Pessoal de Ensino Superior (CAPES), SINAPAD Santos-Dumont, and Federal University of Juiz de Fora (UFJF) for funding this work.

References

[1] Tsao CW, Aday AW, Almarzooq ZI, et al. Heart disease and stroke statistics—2023 update: A report from the american heart association. Circulation 2023;147:e93–e621.

[2] Tomek J, Bueno-Orovio A, Passini E, Zhou X, Minchole A, Britton O, Bartolucci C, Severi S, Shrier A, Virag L, Varro A, Rodriguez B. Development, calibration, and validation of a novel human ventricular myocyte model in health, disease, and drug block. eLife 2019;8:e48890.

[3] Rudy Y. Molecular basis of cardiac action potential repolarization. Annals of the New York Academy of Sciences 2008;1123(1):113–118.

[4] Bueno-Orovio A, Cherry EM, Fenton FH. Minimal model for human ventricular action potentials in tissue. Journal of Theoretical Biology 2008;253(3):544–560.

[5] Keldermann RHea. Effect of heterogeneous apd restitution on vf organization in a model of the human ventricles. American Journal of Physiology Heart and Circulatory Physiology 2008;294(2):H764–H774.

[6] Sobol IM. Sensitivity estimates for nonlinear mathematical models. Mathematical Modelling and Computational Experiments 1993;1(4):407–414.

[7] Saltelli A, Annoni P, Azzini I, Campolongo F, Ratto M, Tarantola S. Variance based sensitivity analysis of model output. Design and estimator for the total sensitivity index. Computer Physics Communications 2010;181(2):259–270.

[8] Deb K, Pratap A, Agarwal S, Meyarivan T. A fast and elitist multiobjective genetic algorithm: NSGA-II. IEEE Transactions on Evolutionary Computation 2002;6(2):182–197.

[9] Lam SK, Pitrou A, Seibert S. Numba: A llvm-based python jit compiler. In Proceedings of the Second Workshop on the LLVM Compiler Infrastructure in HPC, LLVM '15. New York, NY, USA: Association for Computing Machinery. ISBN 978-1-4503-4005-2, 2015; .

[10] Blank J, Deb K. pymoo: Multi-objective optimization in python. IEEE Access 2020;8:89497–89509.

Address for correspondence:

Rodrigo Weber dos Santos
Federal University of Juiz de Fora
rodrigo.weber@ufjf.br